Chemical Engineering Journal 144 (2008) 110–118

Contents lists available at ScienceDirect

Chemical Engineering Journal

journal homepage: www.elsevier.com/locate/cej

# Finite element solution for gas–solid reactions: Application to the moving boundary problems

A. Afshar Ebrahimi [a,*], H. Ale Ebrahim [a], M. Hatam [b], E. Jamshidi [a]

[a] Department of Chemical Engineering, Amirkabir University of Technology (Tehran Polytechnic), Petrochemical Center of Excellency, Tehran 15875-4413, Iran
[b] Department of Mechanical Engineering, Fars Engineering Research Center, Shiraz, Iran

ARTICLE INFO

*Article history:*
Received 4 February 2008
Received in revised form 14 May 2008
Accepted 15 May 2008

*Keywords:*
Gas–solid reactions
Finite element method
Rayleigh–Ritz

ABSTRACT

Gas–solid reactions are very important in the chemical and metallurgical process industries. Several models described these reactions such as volume reaction model, grain model, and nucleation model. These models give two coupled partial differential equations (CPDEs). In this work an integral transformation and subsequent finite element method is used for solving the coupled partial differential equations of these reactions. In each mesh the Rayleigh–Ritz method is applied. Finally the results of this work are compared with the existing numerical solutions and experimental data successfully.



## 1. Introduction

Gas–solid reactions are very important in many chemical and metallurgical processes such as metal oxides reduction [1–3], metal sulfides roasting [4], adsorption of gaseous pollutants [5,6], coal gasification [7], active carbon preparation [8] and catalyst regeneration [9,10]. Reaction engineering of these processes is based on a series of mathematical modeling [11,12]. These models for a porous solid pellet consist of volume reaction model [13–15], the grain model [16–21], random pore model [22–24] and nucleation model [25–28].

The volume reaction model assumes that the reaction and diffusion take place simultaneously in the porous pellet as a homogeneous system [13–14]. When the rate dependency on the solid concentration is below the first order, there is a time for complete of the reaction. After this time, there are two outer diffusion layer and inner diffusion-reaction layer. Therefore, the system becomes to a moving boundary problem with a tedious equations [15]. In this reference the cumulative gas concentration was defined and the orthogonal collocation method was applied for solving the volume reaction model equations.

Moreover, some of the important gas–solid reactions in chemical and metallurgical industries consist of solid pellets produced from small particles or grains [12]. The grain model is a suitable mathematical representation of this system, which assumes that the reaction is accomplished on the surface of the fine and non-porous grains. In many of these gas–solid reactions a solid layer build up around each grain in the form of product or impurities creating another resistance against gas diffusion [11]. The grain model with product layer resistance has been developed for the study of such systems [18].

Nucleation effects are often significant, for example in the reduction of metallic oxides. The conversion–time behavior of these systems at low temperatures shows periods of induction, acceleration, and decay [12], e.g. in the reduction of nickel oxide with hydrogen [1]. A rate equation, in the absence of pore diffusion, has been developed for the interpretation of experimental conversion–time data showing sigmoidal trends [29]. A more general problem has been presented for isothermal and non-isothermal cases [25]. The effect of pore diffusion in the nucleation model has been analyzed by Sohn [26]. A numerical solution and an approximate relation between the conversion and time have also been presented. In Ref. [30], the population balance approach was applied to the cuprous iodide oxidation system. The results of Ref. [31] are in good agreement with the numerical solution of Sohn [26]. Shieh and Lee [32] incorporated induction time using the surface activation concept. Finally, effect of bulk flow for the porous pellets was considered in this model by Sohn and Bascur [33].

In this work, an integral transformation and subsequent Rayliegh–Ritz finite element method is applied to solve the gas–solid reactions equations. The solution technique for the nucleation model (which contains significant non-linear terms) is described in details. Other presented model equations can be solved similarly. Some computer codes have been developed for this purpose in MATLAB media. This program can solve the model equations with various mesh numbers. The number of meshes depends on the

* Corresponding author. Tel.: +98 21 64543198; fax: +98 21 66405847.
*E-mail address:* a.afshar@aut.ac.ir (A.A. Ebrahimi).

1385-8947/$ – see front matter © 2008 Elsevier B.V. All rights reserved.
doi:10.1016/j.cej.2008.05.016

**Nomenclature**

$a = C_A/C_{Ag}$ dimensionless gas concentration
$b = C_B/C_{B0}$ dimensionless solid concentration
$C_A$ gas concentration in the pellet
$C_{Ag}$ bulk gas concentration
$C_B$ solid concentration
$C_{B0}$ initial solid concentration
$D_{AB}$ molecular diffusivity
$D_e$ effective diffusivity of gas A in the pellet
$F_p$ shape factor of the pellet = 1,2,3 for slab, cylinder and sphere, respectively
$h$ length of an element
$i,j$ position indexes
$k$ reaction rate constant for the nucleation model
$k_g$ reaction rate constant for the model presented in Ref. [1]
$k_m$ mass transfer coefficient
$L$ distance from center of the pellet
$M_A$ molecular weight of gaseous reactant
$M_B$ molecular weight of solid reactant
$M_{NiO}$ molecular weight of nickel oxide
$n$ a positive integer in Eq. (14)
$N_{sh} = k_m R/D_e$ Sherwood number
$r_g$ radius of unreacted core in the grain
$r_{g0}$ initial grain radius
$r^* = r_g/r_{g0}$ dimensionless unreacted radius in the grain
$R$ characteristic pellet length
$R_g$ universal gas constant
$t$ time
$T$ absolute temperature (°K)
$X$ solid conversion
$y = L/R$ dimensionless position in the Pellet
$Y$ cumulative gas concentration

*Greek letters*
$\varepsilon$ pellet porosity
$\theta_g = \theta_{pl} = (KC_{Ag}M_B t)/(\rho_B r_{g0})$ dimensionless time for the grain models
$\theta_N = \upsilon_B k C_{Ag} t$ dimensionless time for the nucleation model
$\theta_{vol} = \frac{k C_{Ag} C_{B0}^P}{C_{B0}} t$ dimensionless time for volume reaction model
$\rho_B$ true molar density of solid reactant B
$\sigma = R\sqrt{\frac{F_g K_s (1-\varepsilon)}{D_e r_{g0}}}$ reaction Thiele modulus for the pellet in the grain models
$\sigma_N = R\sqrt{\frac{k \rho_B (1-\varepsilon)}{2 D_e F_p}}$ Thiele modulus for nucleation model
$\sigma_g = \sqrt{\frac{K_s r_{g0}}{2 D_{eg} F_g}}$ reaction modulus for the grain
$\phi = R\sqrt{\frac{k C_{B0}^P}{D_e}}$ reaction Thiele modulus for the volume reaction model
$\upsilon_B$ stoichiometric coefficient of solid reactant
$\tau$ tortuosity factor

gas concentration gradient in the solid pellet, which is determined by Thiele modulus. The preferences of finite element method over other conventional solution techniques in this field are as follows:

1. accuracy,
2. having the profile of the target function between global nodes,
3. capability of imposing various boundary conditions to the problem, and
4. capability of solving these equations in various reaction regimes even in the presence of high concentration gradients.

The results of this method are compared with other solutions and experimental data with a good accuracy for the various gas–solid reaction models.

## 2. Mathematical models

A general gas–solid reaction can be given as

$$A(g) + \upsilon_B B(s) \rightarrow C(g) + \upsilon_D D(s) \quad (1)$$

For a single porous pellet, the following assumptions can be made.

- Pseudo-steady state describes concentration of 'A' in the pellet.
- Equimolar counter-diffusion exists within the pellet.
- The system is isothermal.
- Solid structure is unaffected by the reaction.
- The reaction is irreversible and first order with respect to the gaseous reactant.
- The external mass transfer resistance is negligible.

### 2.1. Nucleation model

The general dimensionless conservation equations of gas and solid, based on nucleation growth kinetics are as follows [26]:

$$\frac{1}{y^{F_p-1}} \frac{\partial}{\partial y}\left(y^{F_p-1} \frac{\partial a}{\partial y}\right) = -2F_p \sigma_N^2 \frac{a}{f'(b)} \quad (2)$$

$$\frac{\partial b}{\partial \theta_N} = \frac{a}{f'(b)} \quad (3)$$

With the initial and boundary conditions

$$\theta_N = 0, \quad b = 1 \quad (4)$$

$$y = 0, \quad \frac{\partial a}{\partial y} = 0 \quad (5)$$

$$y = 1, \quad a = 1 \quad (6)$$

where the dimensionless quantities are defined in the notation, and

$$f'(b) = \frac{\partial f(b)}{\partial b} \quad (7)$$

$$f(b) = [-\ln(b)]^{1/n} \quad (8)$$

These coupled partial differential equations must be solved numerically. An approximate solution based on the law of addition of the reaction and diffusion times has also been presented [26]. Reactions which obey the nucleation model do not have two stage reactions at any position of the pellet.

### 2.2. Simple grain model

The dimensionless governing equations in the general form are [11]:

$$\frac{1}{y^{F_p-1}} \frac{\partial}{\partial y}\left(y^{F_p-1} \frac{\partial a}{\partial y}\right) = \sigma^2 r^{*F_g-1} a \quad (9)$$

$$\frac{\partial r^*}{\partial \theta_g} = -a \quad (10)$$

The initial and boundary conditions are as follows:

$$\theta_g = 0 \quad r^* = 1 \tag{11}$$

$$y = 0 \quad \frac{\partial a}{\partial y} = 0 \tag{12}$$

$$y = 1 \quad a = 1 \tag{13}$$

This model consists of two stages. In the first stage ($\theta < \theta_c$), diffusion of gas "A" and reaction between gas "A" and solid "B" are happening simultaneously. At the time $\theta = \theta_c$ all solid of the outer layer of the pellet has been reacted. Then second stage is started when $\theta > \theta_c$. In this stage the gas diffuses through the completely reacted outer layer of the pellet, in order to reach the diffusion-reaction zone. Thus the grain model becomes a moving boundary problem in the second stage.

### 2.3. Grain model with product layer resistance

The general form of differential equations describing the grain model with product layer resistance is [18]:

$$\frac{1}{y^{F_p-1}}\frac{\partial}{\partial y}\left(y^{F_p-1}\frac{\partial a}{\partial y}\right) = \frac{\sigma^2 r^{*F_g-1} a}{1-\sigma_g^2 q'_{F_g}(r^*)} \tag{14}$$

$$\frac{\partial r^*}{\partial \theta_{pl}} = -\frac{a}{1-\sigma_g^2 q'_{F_g}(r^*)} \tag{15}$$

The initial and boundary conditions of this model are the same as the grain model.

Dimensionless parameters are defined in the appendix and it is known that:

$$q'_{F_g}(r^*) = \frac{\partial q_{F_g}(r^*)}{\partial r^*} \tag{16}$$

where for spherical grains ($F_g = 3$):

$$q_{F_g}(r^*) = 1 - 3r^{*2} + 2r^{*3} \tag{17}$$

As described in the grain model, this model is also a moving boundary system.

### 2.4. Volume reaction model

The dimensionless governing equations describing this model are [15]:

$$\frac{1}{y^{F_p-1}}\frac{\partial}{\partial y}\left(y^{F_p-1}\frac{\partial a}{\partial y}\right) = \phi^2 a b^p \tag{18}$$

$$\frac{\partial b}{\partial \theta_{vol}} = -ab^p \tag{19}$$

The initial and boundary conditions of this model are the same as the nucleation model.

$p$ represents the order of the reaction with respect to solid reactant. If $p \geq 1$ the solid reactant concentration at any position cannot drop to zero in finite time and reaction occurs to some varying extent at all positions within the porous pellet at all times. If $0 \leq p < 1$, the solid reactant can be completely depleted at some positions (pellet surface) after finite time. This leads to the moving boundary type of problem like the grain model and grain model with product layer resistance.

## 3. Integral transformation

First of all, the cumulative gas concentration term is defined as follows [15]:

$$Y(y,\theta) = \int_0^\theta a\,\mathrm{d}\theta \tag{20}$$

Combining Eqs. (2) and (3) gives the following equation:

$$\frac{1}{y^{F_p-1}}\frac{\partial}{\partial y}\left(y^{F_p-1}\frac{\partial a}{\partial y}\right) = -2F_p\sigma_N^2\frac{\partial b}{\partial \theta} \tag{21}$$

Integration of Eq. (21) with respect to time from 0 to $\theta$ with use of Eq. (20) and considering initial condition (4), results in a form given below for the nucleation model:

$$\frac{1}{y^{F_p-1}}\frac{\partial}{\partial y}\left(y^{F_p-1}\frac{\partial Y}{\partial y}\right) = -2F_p\sigma_N^2(b-1) \tag{22}$$

$$y = 0 \quad \frac{\partial Y}{\partial y} = 0 \tag{23}$$

$$y = 1 \quad Y = \theta \tag{24}$$

Integration of Eq. (3) with initial condition (4) gives:

$$Y = [-\ln(b)]^{1/n} \tag{25}$$

Thus, by inverting the above equation, $b$ can be expressed as a function of $Y$ as follows:

$$b = \exp(-Y^n) \tag{26}$$

In this work, these equations are solved for $n = 3$ which is the most complicated case in the nucleation model. For other values of $n$, e.g. ($n = 1$), similar procedure can be repeated to obtain the answers.

By considering $n = 3$, differentiating Eq. (25) with respect to $y$ results in:

$$\frac{\mathrm{d}Y}{\mathrm{d}y} = -\frac{1}{3b}[-\ln(b)]^{-2/3}\frac{\mathrm{d}b}{\mathrm{d}y} \tag{27}$$

## 4. Finite element method

First, consider a typical element $\Omega_e(y_a, y_b)$, whose endpoints have the coordinates $y = y_a$ and $y = y_b$, is isolated from the mesh. In this work developing the algebraic equations using the Rayleigh–Ritz method, which is based on the weak form of the differential equation is applied.

Quadratic Lagrangian polynomial approximation of the solution within a typical finite element $\Omega_e$ is applied as follows [34]:

$$b_h^e = \sum_{j=1}^{3} b_j^e \psi_j^e(y) \tag{28}$$

where $b_j^e$ are the values of the solution $b(y,\theta)$ at the nodes of the finite element $\Omega_e$, and $\psi_j$ are quadratic Lagrangian interpolation functions. The necessary and sufficient number of algebraic relations among the $b_j^e$ can be obtained by recasting differential Eq. (22) in a weighted-integral form ($F_p = 3$):

$$4\pi\int_{y_a}^{y_b} w\left[\frac{1}{y^2}\frac{\partial}{\partial y}\left(y^2\frac{\partial Y}{\partial y}\right) + 6\sigma_N^2 b - 6\sigma_N^2\right] y^2\,\mathrm{d}y = 0 \tag{29}$$

where $w$ denotes the weight function. Terms $4\pi$ and $y^2\,\mathrm{d}y$ in the above equation are due to spherical differential volume element of the pellet which its radius is denoted by $y$. Integrating by parts Eq.

(29) results in:

$$\left[y^2 w \frac{\partial Y}{\partial y}\right]_{y_a}^{y_b} + \int_{y_a}^{y_b} \left(-y^2 \frac{\mathrm{d}w}{\mathrm{d}y}\frac{\mathrm{d}Y}{\mathrm{d}y} + 6\sigma_N^2 y^2 b\, w - 6\sigma_N^2 w y^2\right) \mathrm{d}y = 0 \tag{30}$$

First term in the above equation is related to natural boundary conditions in the nodes of a typical element and is defined as follows in an arbitrary element:

$$Q_1^e = \left(-y^2 \frac{\mathrm{d}Y}{\mathrm{d}y}\right)_{y_1^e}, \quad Q_2^e = \left[\left(y^2 \frac{\mathrm{d}Y}{\mathrm{d}y}\right)_{y_1^{e-}} + \left(-y^2 \frac{\mathrm{d}Y}{\mathrm{d}y}\right)_{y_2^{e+}}\right],$$
$$Q_3^e = \left(y^2 \frac{\mathrm{d}Y}{\mathrm{d}y}\right)_{y_3^e} \tag{31}$$

Substituting Eq. (27) into Eq. (30) gives:

$$\int_{y_a}^{y_b} \left(\frac{1}{3b}[-\ln(b)]^{-2/3} y^2 \frac{\mathrm{d}w}{\mathrm{d}y}\frac{\mathrm{d}b}{\mathrm{d}y} + 6\sigma_N^2 y^2 b\, w\right) \mathrm{d}y = \int_{y_a}^{y_b} 6\sigma_N^2 w y^2 \mathrm{d}y + Q \tag{32}$$

In the Rayleigh–Ritz method we have [34,35]:

$$w = \psi \tag{33}$$

Substituting Eqs. (33) and (28) into Eq. (32) results in:

$$[K^e]\{b^e\} = \{f^e\} + \{Q^e\} \tag{34}$$

where $K^e$ is the coefficient matrix and the column vector $f^e$ is the source vector. These matrices are described as follows [36]:

$$K_{ij}^e = \int_{y_a}^{y_b} \left(y^2 \frac{1}{3\sum_{k=1}^{3} b_k^e \psi_k^e}\left[-\ln\left(\sum_{k=1}^{3} b_k^e \psi_k^e\right)\right]^{-2/3} \frac{\mathrm{d}\psi_i^e}{\mathrm{d}y}\frac{\mathrm{d}\psi_j^e}{\mathrm{d}y} + 6\sigma_N^2 y^2 \psi_i^e \psi_j^e\right) \mathrm{d}y \tag{35}$$

$$f_i^e = \int_{y_a}^{y_b} 6\sigma_N^2 \psi_i^e y^2 \mathrm{d}y \tag{36}$$

The assembly of element equations (Eq. (34)) follows the same procedure as in linear finite element analysis [36]. It should be noted that Eq. (35) does not have analytical solution and must be integrated numerically. This equation contains high non-linear terms also. If we denote the global nodal vector by $\{b\}$, the assembled system of equations can be written as

$$[K(\{b\})]\{b\} = \{F\} \tag{37}$$

where $[K]$ and $\{F\}$ denote the global coefficient matrix and right-hand side vector, respectively. $[K]$ is a non-linear function of the nodal values $b_i$ and it is a $2N+1 \times 2N+1$ symmetric matrix. $N$ is the number of meshes in the domain of the problem. Consequently, the resulting finite element equations are non-linear. It should be noted that all of the global matrix $\{Q\}$ components are zero except the last component. Due to the boundary condition in the center of the pellet first term of this matrix is zero; since there is not any point source or point sink in the domain of the problem, other components of this matrix are also 0.

Since the value of $b_{2N+1}$ is known at the surface of the pellet at each time (see Eq. (26)), the system of equations can be condensed [34]. The condensed non-linear algebraic system of equations is solved by direct iteration technique at each time successfully [36].

**Table 1**
Comparison of the results for nucleation model, for $n=3$ and spherical geometry (small modulus)[a]

| $\theta\downarrow$ | This work F.E.M. | Sohn [26] numerical solution | Sohn [26] approximate solution | Jamshidi and Ale Ebrahim [37] |
|---|---|---|---|---|
| 0.2 | 0.0076 | | | |
| 0.4 | 0.0530 | 0.05 | 0.06 | 0.044 |
| 0.6 | 0.1516 | 0.14 | 0.19 | 0.117 |
| 0.8 | 0.2930 | 0.29 | 0.36 | 0.222 |
| 1 | 0.4600 | 0.46 | 0.52 | 0.351 |
| 1.2 | 0.6145 | 0.62 | 0.66 | 0.494 |
| 1.4 | 0.7496 | 0.75 | 0.76 | 0.64 |
| 1.6 | 0.8516 | 0.87 | 0.83 | 0.779 |
| 1.8 | 0.920 | 0.94 | 0.89 | 0.882 |
| 2 | 0.962 | 0.96 | 0.91 | 0.940 |

[a] $n=3$, $F_p=3$, $\sigma_N=1$.

**Table 2**
Comparison of the results for nucleation model, for $n=1$ and spherical geometry (small modulus)[a]

| $\theta\downarrow$ | This work F.E.M. | Sohn [26] numerical solution | Sohn [26] approximate solution | Jamshidi and Ale Ebrahim [37] |
|---|---|---|---|---|
| 0.2 | 0.1399 | 0.13 | 0.18 | 0.141 |
| 0.4 | 0.268 | 0.26 | 0.32 | 0.267 |
| 0.6 | 0.3705 | 0.37 | 0.42 | 0.381 |
| 0.8 | 0.4644 | 0.46 | 0.51 | 0.482 |
| 1 | 0.5460 | 0.55 | 0.57 | 0.57 |
| 1.2 | 0.6165 | 0.62 | 0.64 | 0.646 |
| 1.4 | 0.6772 | 0.69 | 0.7 | 0.711 |
| 1.6 | 0.7292 | 0.74 | 0.744 | 0.765 |
| 1.8 | 0.7735 | 0.79 | 0.78 | 0.809 |
| 2 | 0.8110 | 0.83 | 0.81 | 0.846 |

[a] $n=1$, $F_p=3$, $\sigma_N=1$.

After calculating the values of $b_j$ at each time, the solid conversion for the nucleation model will be computed as follows:

$$X = 1 - F_p \int_0^1 b\, y^{F_p - 1} \mathrm{d}y \tag{38}$$

By numerical integration (Simpson's 1/3 rule), the conversion of the solid at each time can be obtained.

## 5. Results and discussion

The results of this work (dotted points) are compared with other existing solution methods and experimental works (continuous lines) in the literature as follows.

### 5.1. Comparison with existing solutions

#### 5.1.1. Nucleation model

Comparison of the solid conversions is shown in three conditions.

Table 1 shows the results for $n=3$ and $\sigma=1$. The results of this table are obtained by using the uniform mesh of two quadratic elements, i.e. each mesh has the length of $h=0.5$. Table 2 shows the results for $n=1$ and $\sigma=1$. The results of this table are also obtained by using the uniform mesh of two quadratic elements. Finally in Table 3 the uniform mesh of 40 quadratic elements is used for $n=1$ and $\sigma=10.2$ due to high gas concentration gradients in the pellet (diffusion control regime) and extreme non-linearity in Eq. (37).

Fig. 1 is the comparison of this work with numerical solution of Sohn [26] for $n=3$ and low Thiele modulus. Figs. 2 and 3 are the same comparisons for $n=1$ at low and high Thiele modulus, respectively. In the mentioned cases, dimensionless time step of 0.1 gives accurate results.

**Table 3**
Comparison of the results for nucleation model, for $n = 1$ and spherical geometry (large modulus)[a]

| $\theta\downarrow$ | This work F.E.M. | Dudukovic and Lamba [15] orthogonal collocation | Sohn [26] approximate solution | Jamshidi and Ale Ebrahim [37] |
|---|---|---|---|---|
| 1 | 0.099 | 0.098 | 0.151 | 0.099 |
| 2 | 0.1722 | 0.171 | 0.214 | 0.176 |
| 3 | 0.2237 | 0.224 | 0.262 | 0.237 |
| 4 | 0.2776 | 0.279 | 0.301 | 0.286 |
| 5 | 0.3154 | 0.312 | 0.335 | 0.323 |
| 6 | 0.3562 | 0.350 | 0.364 | 0.352 |
| 7 | 0.3849 | 0.380 | 0.391 | 0.374 |
| 8 | 0.4022 | 0.401 | 0.416 | 0.392 |
| 9 | 0.4288 | 0.430 | 0.739 | 0.407 |
| 10 | 0.4531 | 0.452 | 0.460 | 0.420 |

[a] $n = 1$, $F_p = 3$, $\sigma_N = 10.2$.

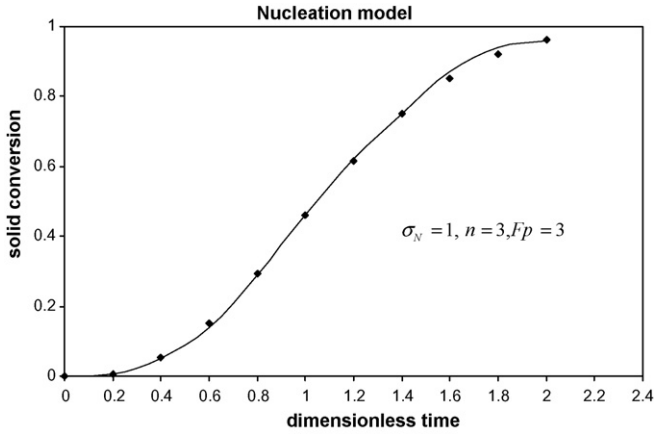


**Fig. 1.** Comparison of this work with numerical solution of Sohn [26] for $n = 3$ and $\sigma_N = 1$.

### 5.1.2. Simple grain model

Fig. 4 is a comparison of this work with the solution of Sohn and Szekely [16], for $F_p = F_g = 3$. Fig. 5 shows comparison between finite element results and the approximate solution of Evans and Rande [38] for $F_p = 3$, $F_g = 2$. Fig. 6 represents comparison between results of this work with results of Sohn and Szekely [16] in the presence of external mass transfer resistance. In this case the boundary condition at the surface of the pellet is as follows:

$$\frac{\partial a}{\partial y} = N_{sh}(1 - a) \tag{39}$$

Integration of Eq. (10) with initial condition (11) gives:

$$Y = 1 - r^* \tag{40}$$

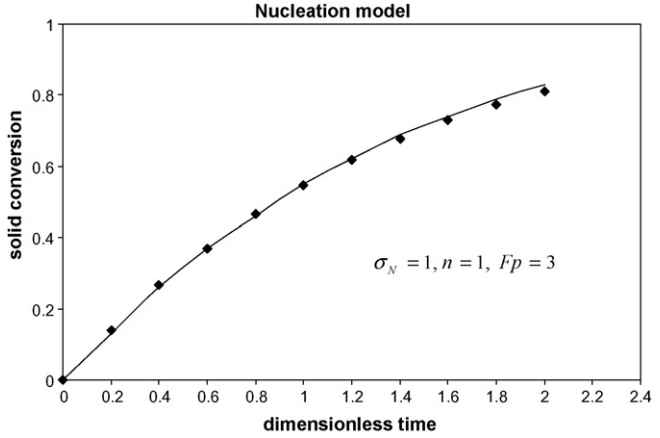


**Fig. 2.** Comparison of this work with numerical solution of Sohn [6] for $n = 1$ and $\sigma_N = 1$.

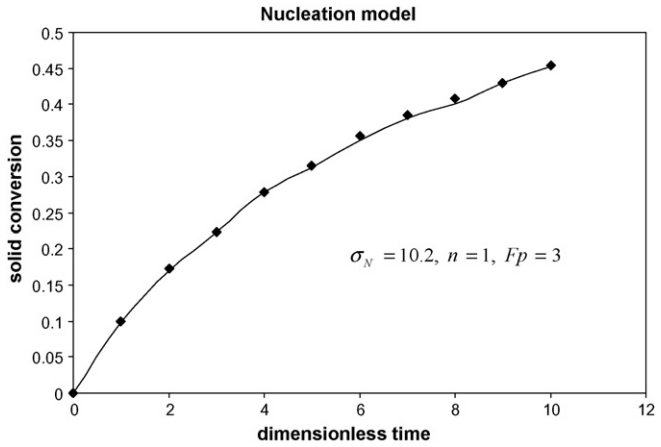


**Fig. 3.** Comparison of this work with numerical solution of Dudukovic and Lamba [11] for $n = 1$ and $\sigma_N = 10.2$.

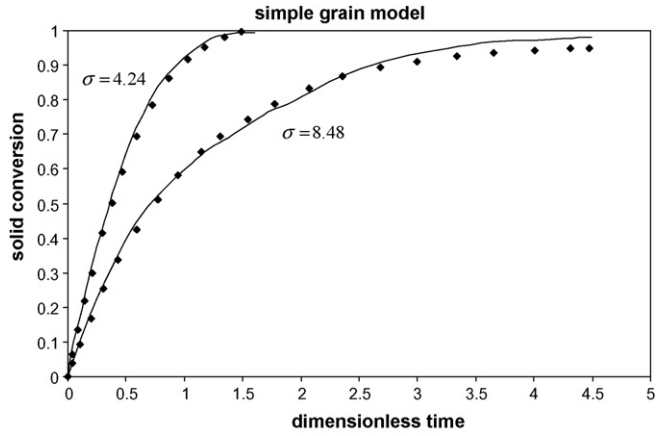


**Fig. 4.** Comparison of this work with numerical solution of Sohn and Szekely [16], for $F_p = F_g = 3$.

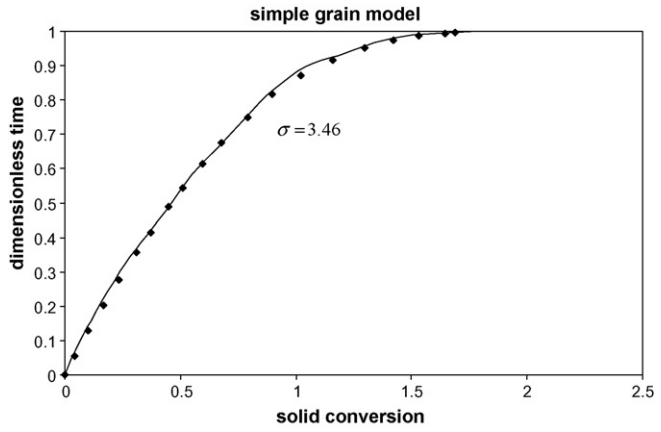


**Fig. 5.** Comparison of results of this work with approximate solution of Evans and Rande [38] for $F_p = 3$, $F_g = 2$.

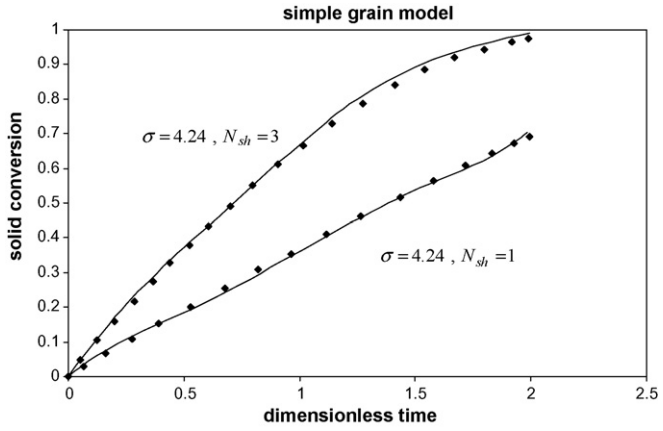


**Fig. 6.** Comparison between results of this work with results of Sohn and Szekely [16] in the presence of external mass transfer resistance for $F_p = F_g = 3$.

The end of the first stage can be found by letting $r^* = 0$ when $y = 1$ and $a = 1$ at the above equation, thus we have $\theta = 1$ for end of the first stage in case of infinite Sherwood number.

When we are in the beginning of second stage of the reaction, the last component of the global nodal vector becomes negative; this does not have a physical meaning in reaction engineering but does have a mathematical meaning. By the progress of reaction, more components of the global nodal vector become negative. This shows the progress of the completely reacted zone toward the center of the pellet (moving boundary behavior). These negative components will be considered zero in calculation of the solid conversion but employing their negative value in calculation of the global nodal vector is necessary at each time. This behavior is repeated in the second stage of grain model with product layer resistance and volume reaction model as well.

### 5.1.3. Grain model with product layer resistance

Results of this work (dotted points) are compared with the numerical solution of Calvelo and Smith [39] in Fig. 7. In this figure comparison of the solid conversions is shown in three reaction regimes. In case of kinetically reaction control regime for the grains ($\sigma_g^2 = 1/6$), the uniform mesh of two quadratic elements is used, i.e. each mesh has the length of $h = 0.5$. In the intermediate regime, i.e. both kinetic and diffusion are significant ($\sigma_g^2 = 10/6$) the uniform

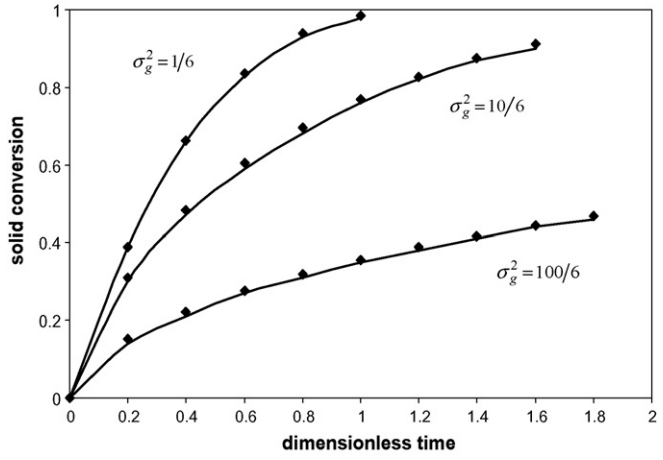


**Fig. 7.** Comparison between results of this work with the numerical solution of Calvelo and Smith [39] for $F_p = F_g = 3$ for the grain model with product layer resistance.

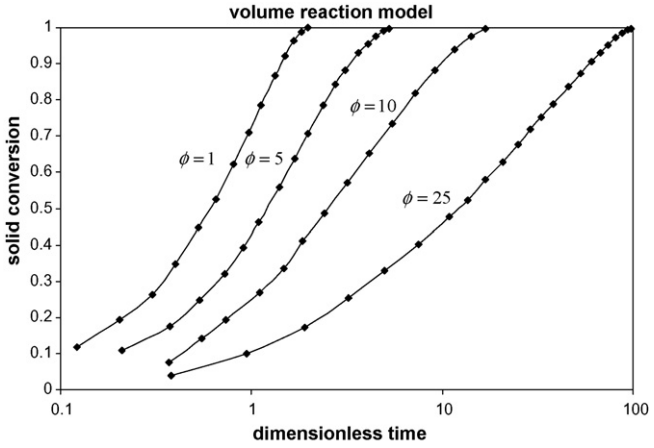


**Fig. 8.** Comparison of this work with numerical solution of Dudukovic and Lamba [15] for spherical pellet in different Thiele modulus.

mesh of three ($h = 1/3$) quadratic elements has been employed and finally in case of completely diffusion control regime ($\sigma_g^2 = 100/6$). Due to steep gas concentration gradients in the solid pellet, uniform mesh of four quadratic elements gives accurate results.

Integration of Eq. (15) with initial condition (11) gives:

$$Y = 1 + \sigma_g^2 - r^* - 3\sigma_g^2 r^{*2} + 2\sigma_g^2 r^{*3} \quad (41)$$

The end of the first stage can be found by letting $r^* = 0$ when $y = 1$ and $a = 1$ at the above equation, thus we have $\theta = 1 + \sigma_g^2$ for the end of the first stage and second stage starts from $\theta > 1 + \sigma_g^2$.

### 5.1.4. Volume reaction model

In Figs. 8 and 9, comparison between finite element solution and orthogonal collocation [15] is considered. Since the reaction order with respect to the solid reactant is 0.5 in this part, we have a two-stage (moving boundary) reaction in these figures. Comparison of the results in different Thiele modulus shows complete agreement between the results of this work and results of Ref. [15].

Integration of Eq. (18) with initial condition at $\theta_{vol} = 0$ $b = 1$ and considering $p = 0.5$ gives:

$$Y = 2(1 - \sqrt{b}) \quad (42)$$

The end of the first stage can be found by letting $b = 0$ when $y = 1$ and $a = 1$ at the above equation, thus we have $\theta = 2$ for the end of

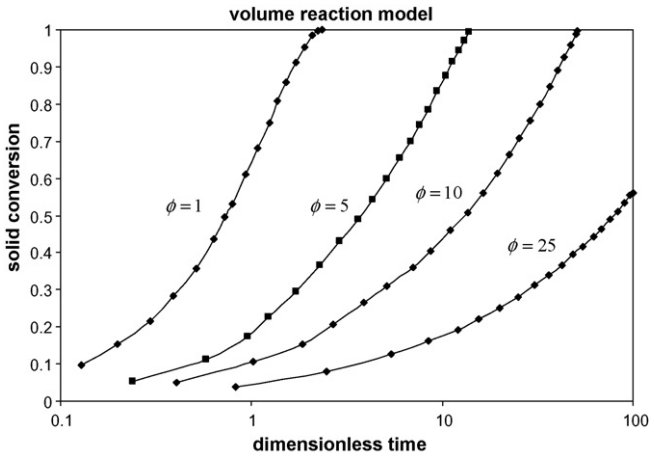


**Fig. 9.** Comparison of this work with numerical solution of Dudukovic and Lamba [15] for slab pellet in different Thiele modulus.

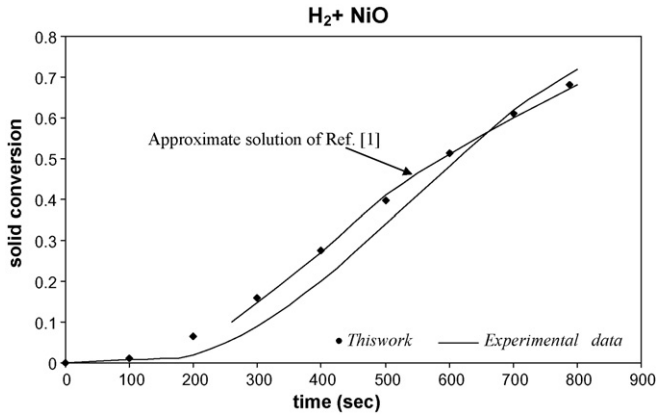


**Fig. 10.** Comparison of this work with experimental work of Szekely and Sohn [2] $T = 520\,^{\circ}$K, $R = 0.21$ cm, $\varepsilon = 0.529$, $n = 3$, $F_p = 1$, $k = 103.02\,\text{cm}^3/\text{gmol s}$ $\tau \approx 2.5$, $D_e \simeq 0.1\,\text{cm}^2/\text{s}$.

the first stage in case of half order reaction with respect to solid reactant.

### 5.2. Comparison with experimental works

#### 5.2.1. Nucleation model

The experimental gas–solid reaction which is considered in this part is as follows:

$$H_2(\text{gas}) + \text{NiO}(\text{solid}) \rightarrow H_2O(\text{gas}) + \text{Ni}(\text{solid}) \quad (43)$$

Most of the assumptions in the mathematical modeling part of this paper are acceptable for the above reaction [1]. The results of two experimental works from Ref. [1] with various temperatures and pellet sizes are compared with finite element results in Figs. 10 and 11 successfully. In Ref. [1] a gas–solid reaction based on the grain model [16–21] has been employed for the reduction of porous nickel oxide pellets with hydrogen. Experimental data of this reaction obtained by Szekely and Sohn [1] is presented in Table 4. Szekely and Sohn [1] obtained the tourtousity and grain radius by minimizing the variance in tourtousity value. The average value of $\tau$ thus found was 2.5 and the corresponding grain size was about 9 μm [1]. Results of this work (finite element method) are obtained by employing the experimental data of Table 4.

In this work we shall change the grain model reaction rate constant into nucleation model reaction rate constant. This procedure

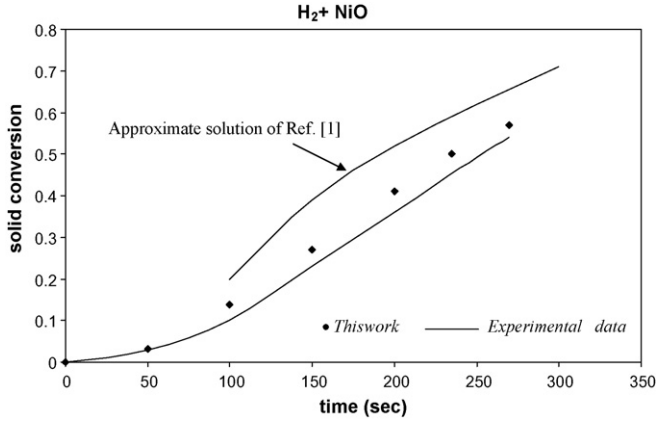


**Fig. 11.** Comparison of this work with experimental work of Szekely and Sohn [2] $T = 552\,^{\circ}$K, $R = 0.21$ cm, $\varepsilon = 0.53$, $n = 3$, $F_p = 1$, $k = 335.9\,\text{cm}^3/\text{gmol s}$, $\tau \approx 2.5$, $D_e \simeq 0.1\,\text{cm}^2/\text{s}$.

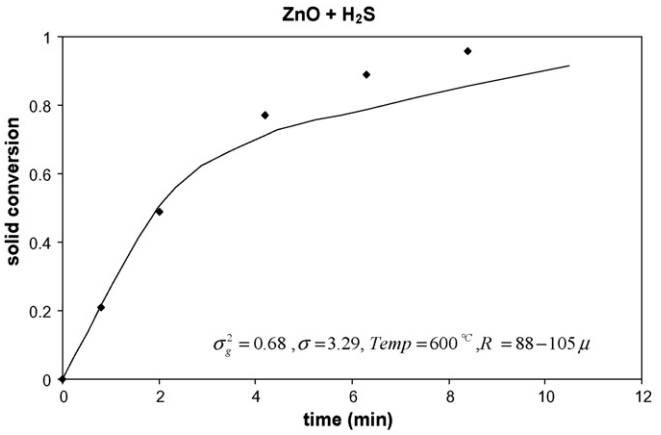


**Fig. 12.** Comparison of this work (dotted points) with experimental data (continuous line) of Efthimiadis and Sotirchos [6].

**Table 4**
Experimental operating conditions for the reduction of nickel oxide with hydrogen reported by Szekely and Sohn [1]

| $T\,(^{\circ}\text{K})$ | $F_p$ | $R\,(\text{cm})$ | $\varepsilon$ | $D_{AB}\,(\text{cm}^2/\text{s})$ | $D_e\,(\text{cm}^2/\text{s})$ | $k_g/r_g\,(\text{s}^{-1})$ |
|---|---|---|---|---|---|---|
| 520 | 1 | 0.30 | 0.529 | 2.41 | 0.107 | 9.2 |
| 552 | 1 | 0.21 | 0.53 | 2.65 | 0.112 | 30.0 |

is illustrated in the next equation:

$$k = \frac{k_g M_{\text{NiO}}}{\rho_B r_g} \quad (44)$$

Effective diffusivity coefficient is necessary for calculation of reaction Thiele modulus. This coefficient is obtained by the following equation:

$$\frac{1}{D_e} = \frac{\tau}{\varepsilon}\left(\frac{1}{D_{AB}} + \frac{1}{D_k}\right) \quad (45)$$

where $D_k$ is the Knudsen diffusivity and it is calculated by the following relation:

$$D_k = \frac{r_g}{(1-\varepsilon)(1+\pi/8)(8M_A/\pi R_g T)^{1/2}} \quad (46)$$

In Figs. 10 and 11, the approximate results of Ref. [1] do not obey the trend of experimental data. Moreover, approximate solution of Ref. [1] does not contain any information about the first period (induction time) of such sigmoidal conversion behaviors.

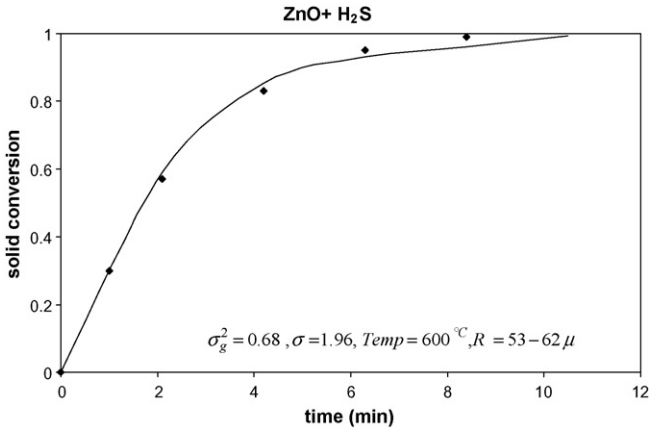


**Fig. 13.** Comparison of this work (dotted points) with experimental data (continuous line) of Efthimiadis and Sotirchos [6].

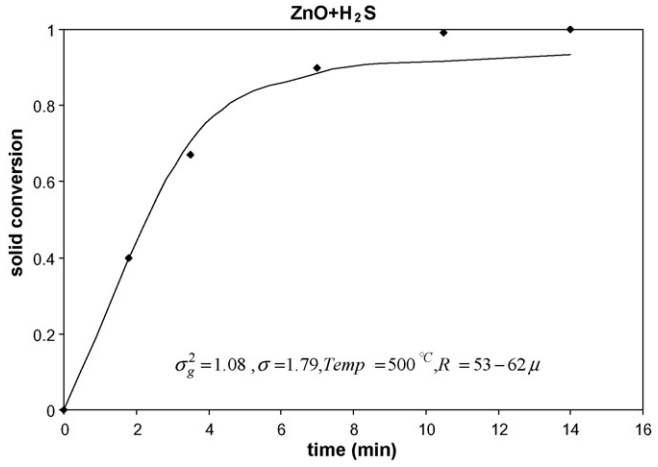


**Fig. 14.** Comparison of this work (dotted points) with experimental data (continuous line) of Efthimiadis and Sotirchos [6].

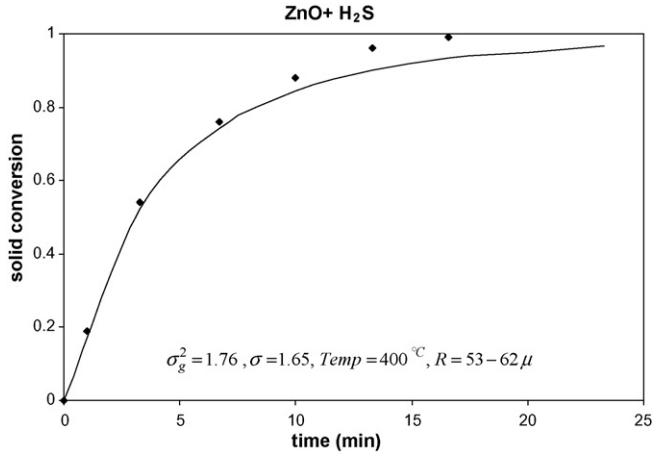


**Fig. 15.** Comparison of this work (dotted points) with experimental data (continuous line) of Efthimiadis and Sotirchos [6].

### 5.2.2. Grain model with product layer resistance

The ZnO + $H_2S$ is an important reaction in petrochemical plants for complete natural gas desulphurization [21,40]. Trace of $H_2S$ is a serious poison for the catalysts of the synthesis reactions. Thus the gas–solid reaction (ZnO + $H_2S$) plays a significant role in removing trace of $H_2S$. Results of finite element method (dotted points) are compared with experimental data (continuous lines) of Efthimiadis and Sotirchos [6]. Comparisons of this work and experimental data of Efthimiadis and Sotirchos [6] are presented in Figs. 12–15 successfully. In these figures effects of pellet size and temperature are considered.

## 6. Conclusion

In this work, a new numerical solution technique has been used for calculating the conversion of four gas–solid reaction models named nucleation model, simple grain model, grain model with product layer resistance and volume reaction model. In the case of comparison with existing numerical solutions, different reaction regimes have been considered for the above gas–solid reaction models. Comparison of results shows a very good agreement between finite element results and other existing solutions. Moreover, this method (Rayleigh–Ritz finite element) reveals very accurate results for the moving boundary problems such as grain models and half order volume reaction model. In the case of comparison with experimental works, results of this novel method show acceptable trend and agreement with experimental data. Thus this new numerical technique can be applied in all reaction regimes successfully. In addition to this, a proper gas–solid reaction model with an accurate solution technique can be applied for predicting the complete behavior of special reactions such as $H_2$ + NiO or $H_2S$ + ZnO successfully. The results of this work can be used for estimating kinetic parameters of such reactions by comparison with experimental data.

## References

[1] J. Szekely, C.I. Lin, H.Y. Sohn, A structural model for gas–solid reactions with a moving boundary. V. An experimental study of the reduction of porous nickel-oxide pellets with hydrogen, Chem. Eng. Sci. 28 (1973) 1975–1989.
[2] K.L. Breg, S.E. Olsen, Kinetics of manganese ore reduction by carbon monoxide, Met. Mater. Trans. B 31 (2000) 477–490.
[3] H. Ale Ebrahim, E. Jamshid, Kinetic study and mathematical modeling of the reduction of ZnO–PbO mixtures by methane, Ind. Eng. Chem. Res. 44 (2005) 495–504.
[4] S. Kimura, Oxidation kinetics of polycrystalline zinc sulfide grains, AIChE J. 35 (1989) 339–342.
[5] S. Zarkanitis, S.V. Sotirchos, Pore structure and particle size effect on limestone capacity for $SO_2$ removal, AIChE J. 35 (1989) 821–830.
[6] E.A. Efthimiadis, S.V. Sotirchos, Reactivity evolution during sulfidation of porous zinc oxide, Chem. Eng. Sci. 48 (1993) 829–843.
[7] E.A. Delikouras, D.D. Perlmuter, Combined effects of mass transfer and inaccessible porosity in gasification reactions, AIChE J. 39 (1993) 829–835.
[8] G.Q. Lu, D.D. Do, A kinetic study of coal reject derived char activation with $CO_2$, $H_2O$ and air, Carbon 30 (1992) 21–29.
[9] P.A. Ramachandran, M.H. Rashid, R. Hughes, A model for coke oxidation from catalyst pellets in the initial burning period, Chem. Eng. Sci. 30 (1975) 1391–1398.
[10] D. Bai, J.X. Zhu, Y. Jin, Z. Yu, Simulation of FCC catalyst regeneration in a riser regenerator, Chem. Eng. J. 71 (1998) 97–109.
[11] J. Szekely, J.W. Evans, H.Y. Sohn, Gas–Solid Reactions, Academic Press, New York, 1976.
[12] P.A. Ramachandran, L.K. Doraiswamy, Modeling of noncatalytic gas–solid reactions, AIChE J. 28 (1982) 881–900.
[13] C.Y. Wen, Noncatalytic heterogeneous solid–fluid reaction models, Ind. Eng. Chem. 60 (1968) 34–54.
[14] M. Ishida, C.Y. Wen, Comparison of kinetic and diffusional models for solid–gas reactions, AIChE J. 14 (1968) 311–317.
[15] M.P. Dudukovic, H.S. Lamba, Solution of moving boundary problems for gas–solid noncatalytic reactions by orthogonal collocation, Chem. Eng. Sci. 33 (1978) 303–314.
[16] H.Y. Sohn, J. Szekely, A structural model for gas–solid reactions with a moving boundary. III. A general dimensionless representation of the irreversible reaction between a porous solid and a reactant gas, Chem. Eng. Sci. 27 (1972) 763–778.
[17] J. Szekely, J.W. Evans, Studies in gas–solid reactions. Part I. A structural model for the reaction of porous oxides with a reducing gas, Met. Trans. 2 (1971) 1691–1698.
[18] H.Y. Sohn, J. Szekely, The effect of intragrain diffusion on the reactivity between a porous solid and a gas, Chem. Eng. Sci. 29 (1974) 630–634.
[19] O. Garza-Garza, M.P. Dadukovic, A variable size grain model for gas–solid reactions with structural changes, Chem. Eng. J. 24 (1982) 35–45.
[20] C. Georgakis, C.W. Change, J. Szekely, A changing grain size model for gas–solid reactions, Chem. Eng. Sci. 34 (1979) 1072–1075.
[21] P.V. Ranade, D.P. Harrison, The variable property grain model applied to the zinc oxide–hydrogen sulfide reaction, Chem. Eng. Sci. 36 (1981) 1079–1089.
[22] S.K. Bhatia, D.D. Perlmutter, A random pore model for fluid–solid reactions. I. Isothermal, kinetic control, AIChE J. 26 (1980) 379–386.
[23] S.K. Bhatia, D.D. Perlmutter, A random pore model for fluid–solid reactions. II. Diffusion and transport effects, AIChE J. 27 (1981) 247–254.
[24] S.K. Bhatia, D.D. Perlmutter, The effect of pore structure on fluid–solid reactions: application to the $SO_2$–lime reaction, AIChE J. 27 (1981) 226–234.
[25] E. Ruckestein, T. Vavanellos, Kinetics of solid phase reactions, AIChE J. 21 (1975) 756–763.
[26] H.Y. Sohn, The law of additive reaction time in fluid–solid reactions, Metall. Trans. B 9 (1978) 89–96.
[27] D.J. McCarthy, On the applicability of the nucleation model for oxidation of carbons, Carbon 31 (1993) 63–69.
[28] R. Dziembaj, J. Malczyk, A. Baranski, Oxygen corrosion of calcined cokes. II. Nonlinear nucleation model of this oxygen corrosion, Carbon 29 (1991) 329–334.
[29] M. Avrami, Granulation, phase change, and microstructural kinetics of phase change III, J. Chem. Phys. 9 (1941) 177–184.

[30] S.K. Bhatia, D.D. Perlmutter, A population balance approach to the modeling of solid phase reactions, AIChE J. 25 (1979) 298–306.
[31] P.C. Prasannan, P.A. Ramachandran, L.K. Doraiswamy, Gas–solid reactions: a method of direct solution for solid conversion profiles, Chem. Eng. J. 33 (1986) 19–25.
[32] M.D. Shieh, C. Lee, A more general structural model which includes the induction time for gas–solid reactions. I. Nonporous solids, Chem. Eng. Sci. 47 (1992) 4017–4025.
[33] H.Y. Sohn, O.A. Bascur, Effect of bulk flow due to volume change in the gas phase on gas–solid reactions: initially porous solids, Ind. Eng. Chem. Process Des. Dev. 21 (1982) 658–663.
[34] J.N. Reddy, An Introduction to the Finite Element Method, McGraw-Hill, New York, 2006.
[35] A.W. Leissa, The historical bases of the Rayleigh and Ritz methods, J. Sound Vibration 287 (2005) 961–978.
[36] J.N. Reddy, An Introduction to Nonlinear Finite Element Analysis, Oxford University Press, New York, 2004.
[37] E. Jamshidi, H. Ale Ebrahim, A quantized solution for the nucleation model in gas–solid reactions, Chem. Eng. J. 68 (1997) 1–6.
[38] J.W. Evans, M.G. Rande, The grain model for reaction between a gas and a porous solid—a refined approximate solution to the equations, Chem. Eng. Sci. 35 (1980) 1261–1262.
[39] A. Calvelo, J.M. Smith, Intrapellet transport in gas–solid non-catalytic reactions, Proceedings of the Chemca 70, Butterworth, Australia, 1971, Paper 3.1.
[40] J.B. Gibson, D.P. Harrison, The reaction between hydrogen sulfide and spherical pellets of zinc oxide, Ind. Eng. Chem. Process Des. Dev. 19 (1980) 231–237.